Electric Current Sensors: Analysis of Coreless and Gapped Core Sensors

Noby George, Department of Measurement,
Faculty of Electrical Engineering,
Czech Technical University, Prague

Supervisor: Prof. Pavel Ripka

Czech Technical University in Prague, Faculty of Electrical Engineering

Department of Measurement

Date: 08-06-2023
Time: 10.15-10.30 A.M

Magnetic field sensor based coreless current measurement in rectangular busbar

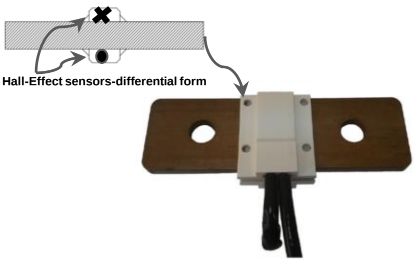

Fig. 1. Hall-effect based differential sensor arrangement for busbar current sensing [1]

[1] M. Blagojević, U. Jovanović, I. Jovanović, D. Mančić, and R. S. Popović, "Realization and optimization of bus bar current transducers based on Hall effect sensors," Meas. Sci. Technol., vol. 27, no. 6, May 2016, Art. no. 65102.

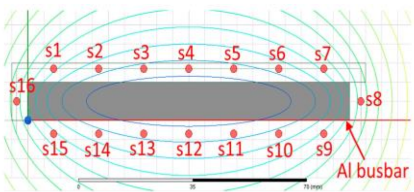

Fig. 3. Rectangular array of fluxgate sensors for current measurement [3].

[3] Ripka, P.; Mlejnek, P.; Hejda, P.; Chirtsov, A.; Vyhnánek, J. Rectangular Array Electric Current Transducer with Integrated Fluxgate Sensors. *Sensors* 2019.

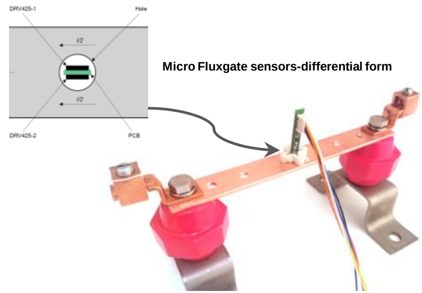

Fig. 2. Micro Fluxgate sensors are arranged in differential form inside a hole in the busbar [2].

[2] "DRV425," *DRV425 data sheet, product information and support | TI.com*. [Online]. Available: https://www.ti.com/product/DRV45.

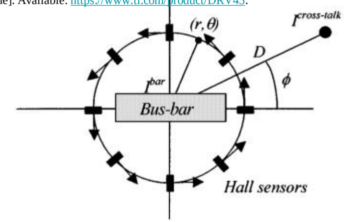

Fig. 4. Circular array of sensors for current measurement [4].

[4] L. Di Rienzo, R. Bazzocchi and A. Manara, "Circular arrays of magnetic sensors for current measurement," in *IEEE Transactions on Instrumentation and Measurement*, vol. 50, no. 5, pp. 1093-1096, Oct. 2001, doi: 10.1109/19.963165.

Frequency dependency busbar current transducers

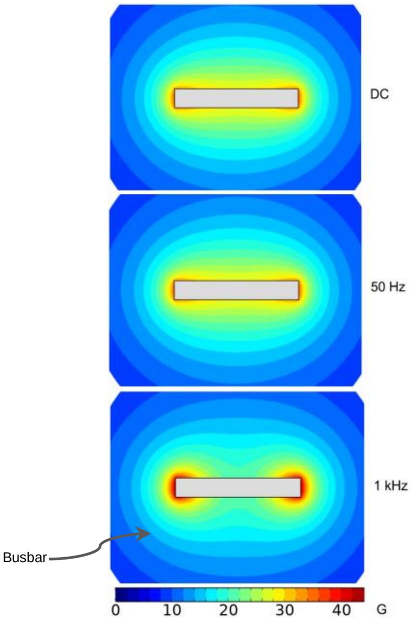

Fig. 5. Magnetic flux density around the rectangular busbar at different frequencies [5].

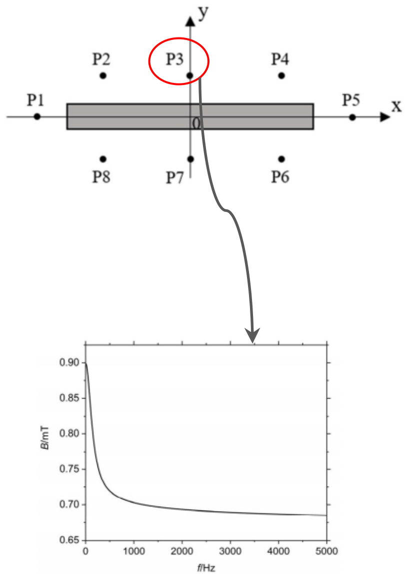

Fig. 6. Change in magnitude of flux density at single sensor location at different frequencies [6].

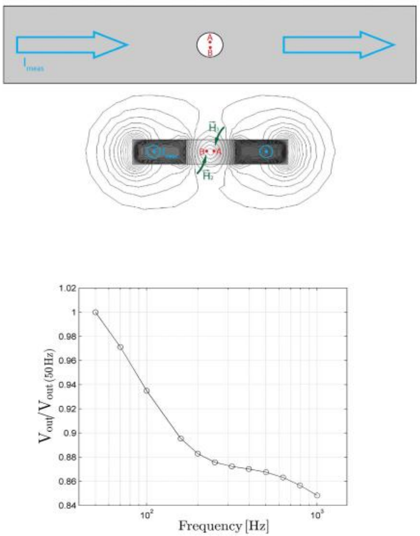

Fig. 7. The busbar current measurement with differential fluxgate sensor (in the centre of the bus bar) and its frequency characteristics [7].

[5] X. P. Xu, S. Wang, T. Z. Liu, M. Zhu and J. G. Wang, "TMR Busbar Current Sensor With Good Frequency Characteristics," in *IEEE Transactions on Instrumentation and Measurement*, vol. 70, pp. 1-9, 2021.

[6] W. Li, G. Zhang, H. Zhong and Y. Geng, "A Wideband Current Transducer Based on an Array of Magnetic Field Sensors for Rectangular Busbar Current Measurement," in *IEEE Transactions on Instrumentation and Measurement*, vol. 70, pp. 1-11, 2021.

[7] P. Ripka, M. Pribil, V. Petrucha *et al.*, "A Fluxgate Current Sensor With an Amphitheater Busbar," *IEEE Transactions on Magnetics*, vol. 52, no. 7, Jul, 2016.

Circular array based coreless current transducer

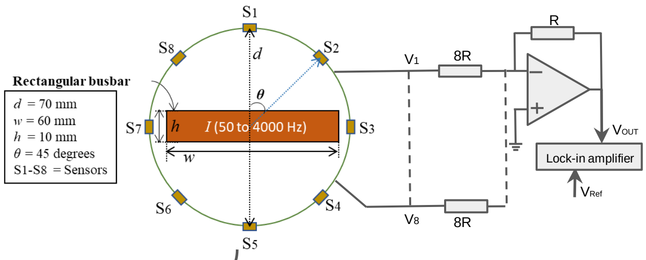

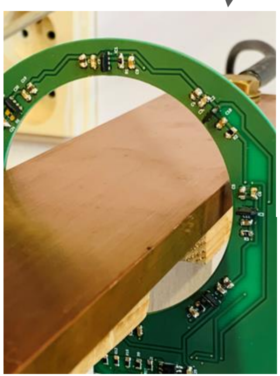

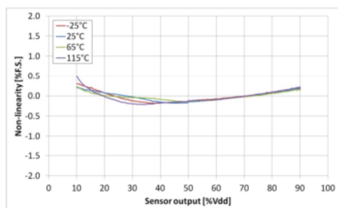

MLX91209- Hall-effect sensor

Bandwidth: DC-250 kHz
Sensing Range: up to 450 mT

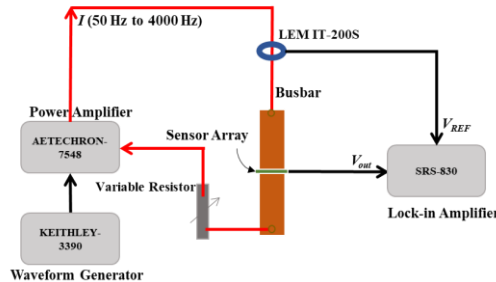

Fig. 10. The experimental setup to study the frequency characteristics of the transducer.

Fig. 9. The circular array of magnetic field sensors for measurement of current in rectangular busbar.

Circular array based coreless current transducer

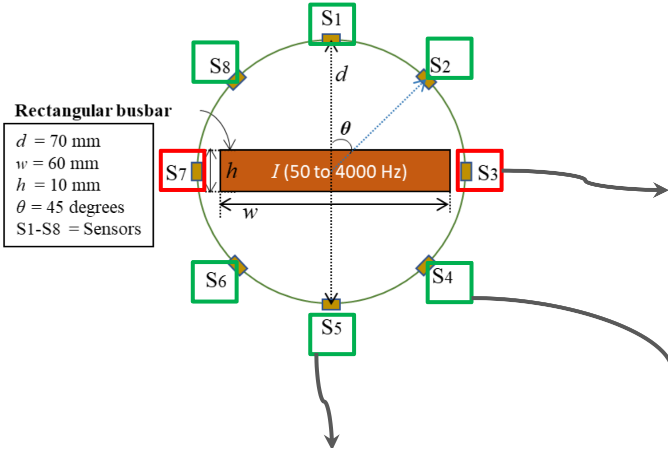

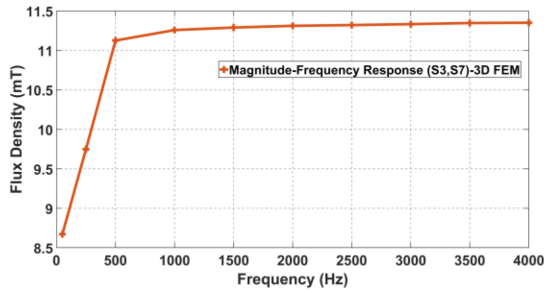

Fig. 11. The magnitude-frequency response of S3 & S7.

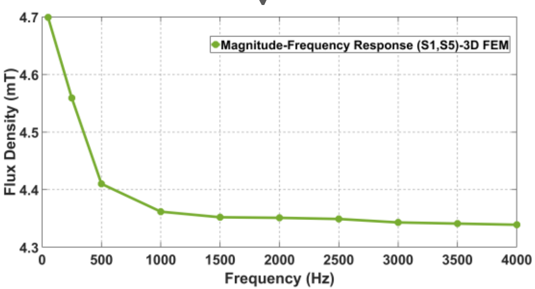

Fig. 12. The magnitude-frequency response of S1 & S5.

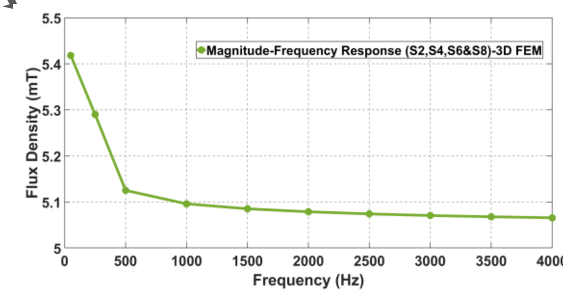

Fig. 13. The magnitude-frequency response of S2, S4, S6 & S8.

Circular array based coreless current transducer

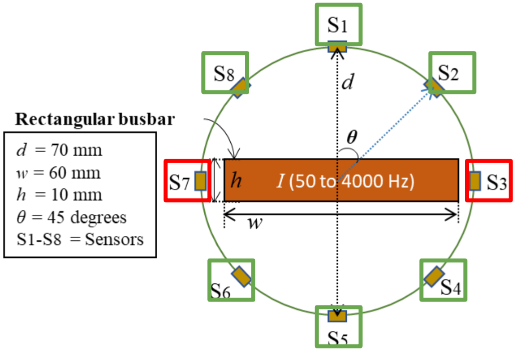

$$Error\ (\%) = \frac{V_{OUT\ (f)} - V_{OUT\ (50Hz)}}{V_{OUT\ (50Hz)}} \times 100$$

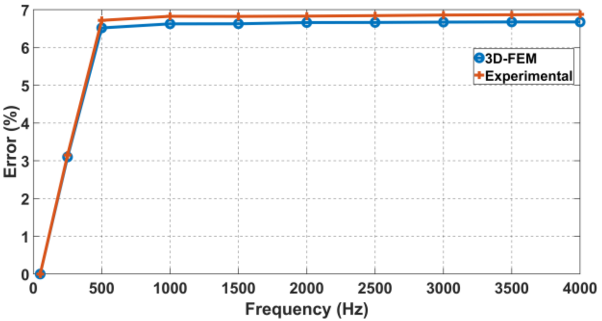

Fig. 14. The frequency characteristics of the circular array-based transducer. The error (%) is the average of the total error contributed by all the sensors in the array.

Improved circular array based coreless current transducer

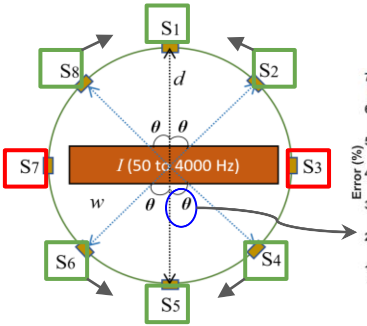

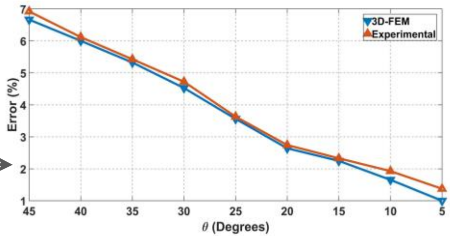

Fig. 15. The average of the total error contributed by all the sensors in the array for different offset angles.

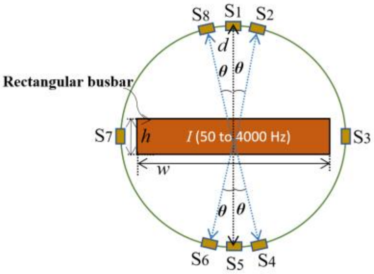

Fig. 16. The improved circular array-based current transducer for rectangular busbar.

Fig. 17. The prototype of the improved circular array-based current transducer for rectangular busbar.

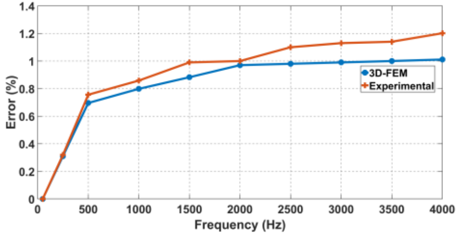

Fig. 18. The frequency characteristics of the improved circular array-based transducer.

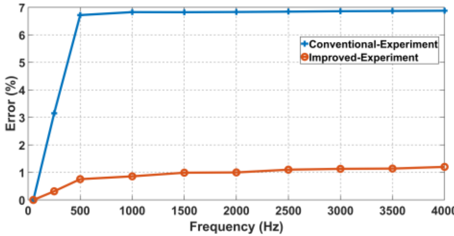

Fig. 19. The frequency characteristics of the improved and conventional circular array-based transducer.

Circular array-based coreless current transducer- Effect of external field

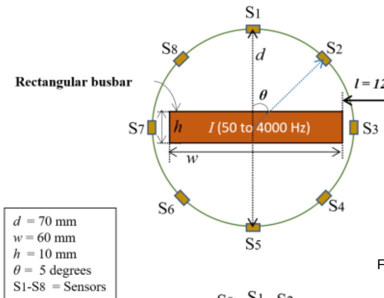

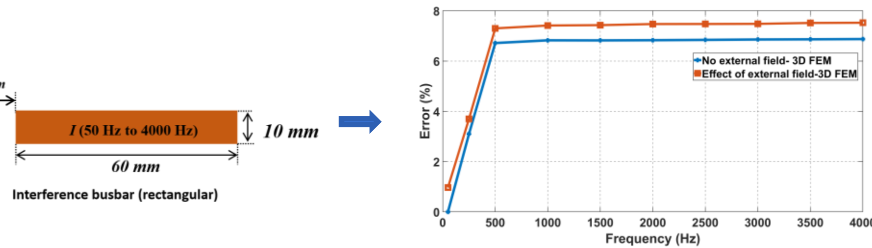

Fig. 20. The effect of an external field on the conventional circular array-based current transducer.

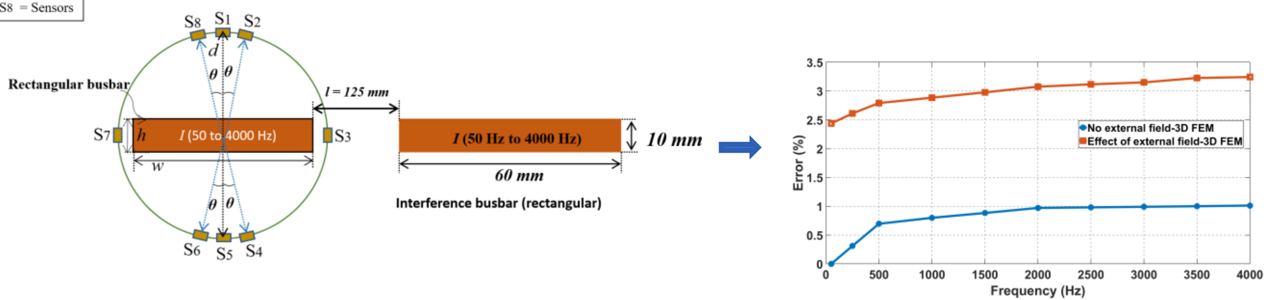

Fig. 21. The effect of an external field on the improved circular array-based current transducer.

Crosstalk in gapped core current sensor: Preliminary results

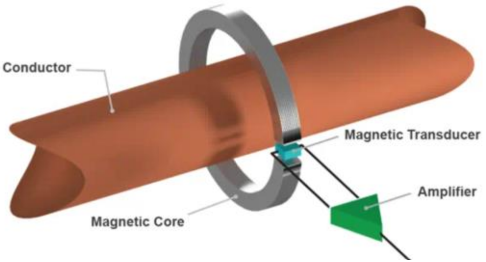

Fig. 22. The gapped core current transducer*. * Picture Courtesy: Allegro Microsystems

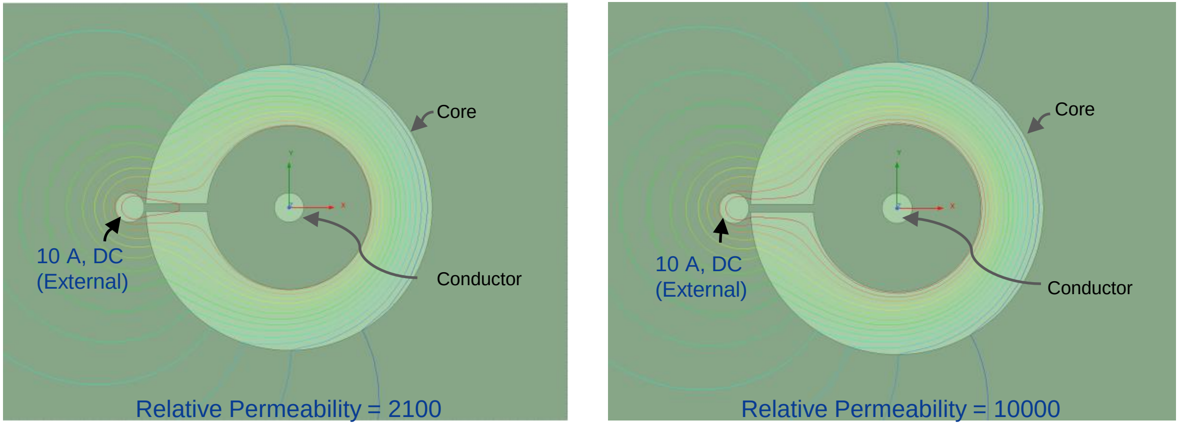

Fig. 23. The effect of the permeability of the core on the crosstalk effect.

Crosstalk in gapped core current sensor

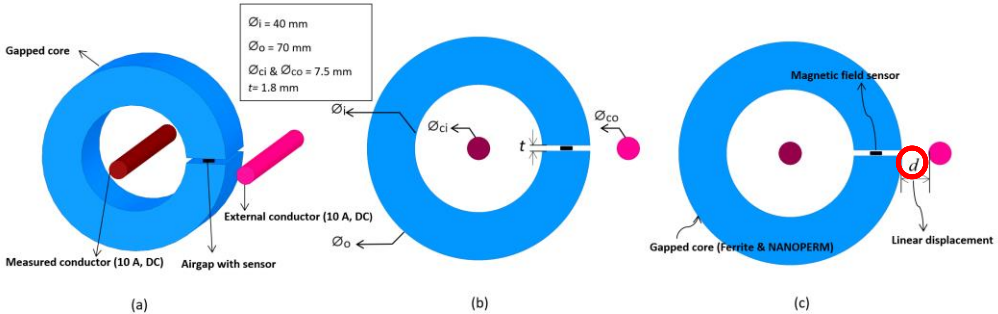

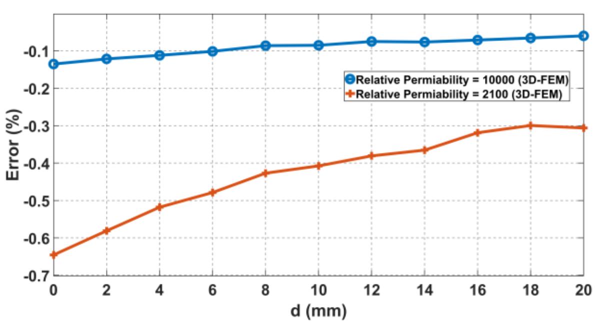

Fig. 24. Crosstalk error characteristics for ferrite and Nanoperm core for linear displacement of the external conductor.

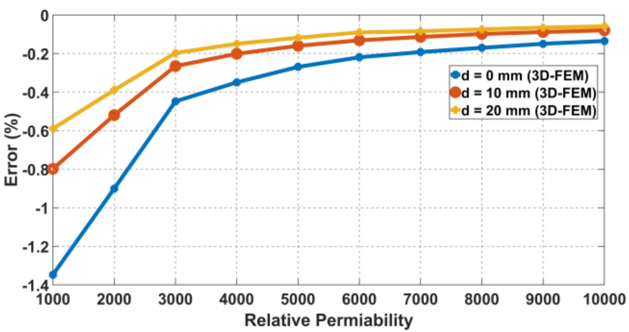

Fig. 25. The crosstalk error for various relative permeability of the gapped core.

Crosstalk in gapped core current sensor

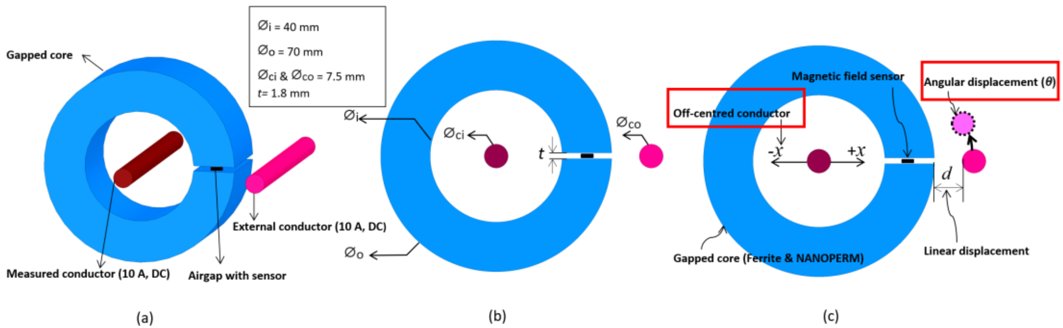

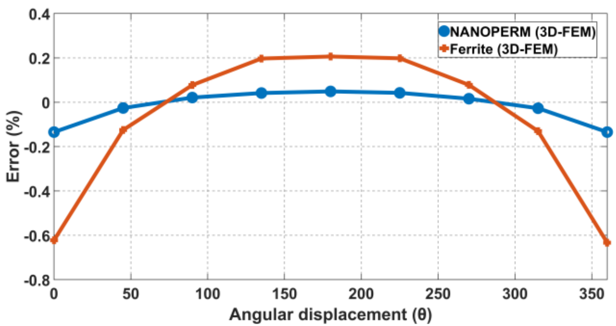

Fig. 26. Crosstalk error at different angular positions of the external conductor.

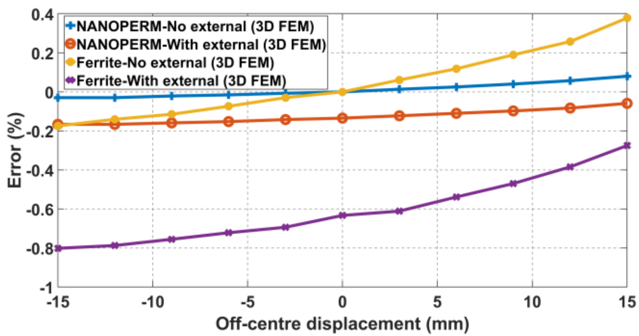

Fig. 27. The effect of off-centered measured conductor on crosstalk by the external conductor.

Crosstalk in dual gapped core current sensor

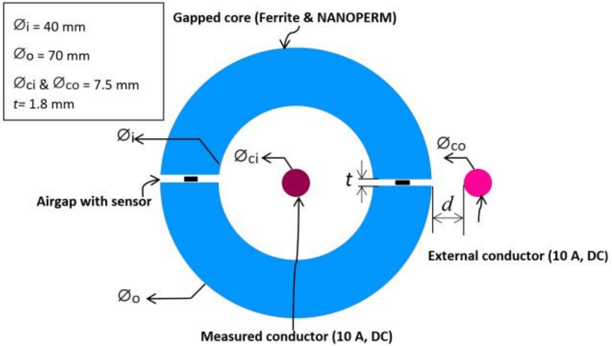

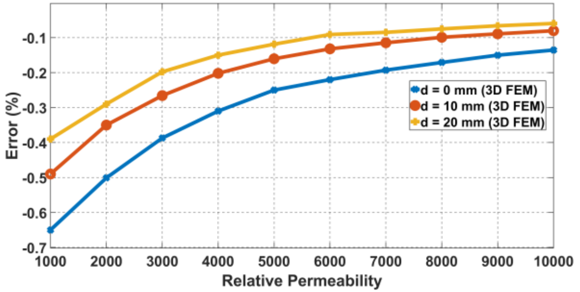

Fig. 29. The dependency of the dual gap current sensor on the external current-carrying conductor, and on the relative permeability of the core.

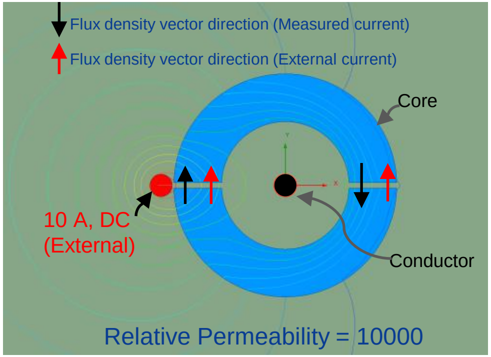

Fig. 28. The gapped core current sensor with two gaps in the core.

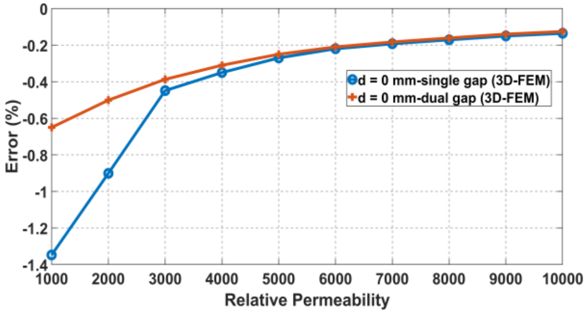

Fig. 30. The comparison of the crosstalk in the single and dual gapped core current transducer.

Conclusions

- The frequency dependency of circular array-based current transducer for rectangular busbar can be improved by adjusting the offset angle between the sensors.
- The frequency dependency of rectangular busbar current sensors can be reduced from 7.00% to 1.2 % at 4 kHz using the proposed busbar configuration.
- Disadvantage - decreased resistance to external fields.

- The crosstalk effect in an open loop single-gapped core current transducer depends on the core's relative permeability and the position of the external conductor.
- The dual-gapped core current transducer showed better (compared to single gap) resistance to the external field for cores with relative permeability less than 6000.

NÁZEV PROJEKTU

Výzva 02_18_053 Mezinárodní mobilita výzkumných, technických a administrativních pracovníků výzkumných organizací

ANGLICKÝ NÁZEV

International mobility of research, technical and administrative staff of research organizations

Project´s number: CZ.02.2.69/0.0/0.0/18_053/0016980

EVROPSKÁ UNIE
Evropské strukturální a investiční fondy
Operační program Výzkum, vývoj a vzdělávání

MINISTERSTVO ŠKOLSTVÍ, MLÁDEŽE A TĚLOVÝCHOVY

ČVUT
ČESKÉ VYSOKÉ UČENÍ TECHNICKÉ V PRAZE

Thank you !